




Aging related impairment of brain microvascular bioenergetics involves oxidative phosphorylation and glycolytic pathways

Siva SVP Sakamuri¹, Venkata N Sure¹, Lahari Kolli¹, Wesley R Evans^{1,2}, Jared A Sperling¹, Gregory J Bix^{2,3}, Xiaoying Wang^{2,3}, Dmitriy N Atochin⁴, Walter L Murfee⁵, Ricardo Mostany^{1,2} and Prasad VG Katakam^{1,2,3} 

Abstract

Mitochondrial and glycolytic energy pathways regulate the vascular functions. Aging impairs the cerebrovascular function and increases the risk of stroke and cognitive dysfunction. The goal of our study is to characterize the impact of aging on brain microvascular energetics. We measured the oxygen consumption and extracellular acidification rates of freshly isolated brain microvessels (BMVs) from young (2–4 months) and aged (20–22 months) C57Bl/6 male mice. Cellular ATP production in BMVs was predominantly dependent on oxidative phosphorylation (OXPHOS) with glucose as the preferred energy substrate. Aged BMVs exhibit lower ATP production rate with diminished OXPHOS and glycolytic rate accompanied by increased utilization of glutamine. Impairments of glycolysis displayed by aged BMVs included reduced compensatory glycolysis whereas impairments of mitochondrial respiration involved reduction of spare respiratory capacity and proton leak. Aged BMVs showed reduced levels of key glycolysis proteins including glucose transporter 1 and 6-phosphofructo-2-kinase/fructose-2,6-biphosphatase 3 but normal lactate dehydrogenase activity. Mitochondrial protein levels were mostly unchanged whereas citrate synthase activity was reduced, and glutamate dehydrogenase was increased in aged BMVs. Thus, for the first time, we identified the dominant role of mitochondria in bioenergetics of BMVs and the alterations of the energy pathways that make the aged BMVs vulnerable to injury.

Keywords

Oxygen consumption rate, oxidative phosphorylation, glycolysis, extracellular acidification rate, ATP

Received 29 June 2021; Revised 16 October 2021; Accepted 19 November 2021

Introduction

Aging impairs cerebrovascular function thereby increasing the risk of stroke.¹ Cerebral microvasculature provides the blood flow to the neuronal tissue and is critical for nutrient transport, neurovascular coupling (NVC), and the maintenance of the blood-brain-barrier (BBB). Aging is associated with the altered microvascular structure, density, and plasticity² that contribute to the microvascular dysfunction including impaired NVC and BBB.^{3,4} Furthermore, cerebrovascular endothelial cells have been shown to mediate the aging-associated circulatory cues on the brain.⁵

¹Department of Pharmacology, Tulane University School of Medicine, New Orleans, LA, USA

²Neuroscience Program, Tulane Brain Institute, Tulane University, New Orleans, LA, USA

³Clinical Neuroscience Research Center, New Orleans, LA, USA

⁴Cardiovascular Research Center, Division of Cardiology, Department of Medicine, Massachusetts General Hospital, Harvard Medical School, Charlestown, MA, USA

⁵J. Crayton Pruitt Family Department of Biomedical Engineering, University of Florida, Gainesville, FL, USA

Corresponding author:

Prasad VG Katakam, 1430 Tulane Avenue, Room 3554C, Mail Code 8683, New Orleans, LA 70112, USA.
Email: pkatakam@tulane.edu

Maintenance of BBB integrity, NVC function, and steady nutrient support are energy-demanding processes for cerebral microvasculature. Optimal functioning of energy pathways, including glycolysis and mitochondrial oxidative phosphorylation (OXPHOS), is required for meeting the energy demands of cells. Brain microvessels (BMVs) are comprised of three types of blood vessels, namely, precapillary arterioles, capillaries, and post-capillary venules.^{6–9} Capillaries contain predominantly endothelial cells along with a few pericytes whereas precapillary arterioles and venules also contain smooth muscle cells. The functioning of all the microvascular cells is modulated by interactions with neurons and astrocytes.¹⁰

Previous studies have shown that glycolysis is the primary source of ATP generated in non-cerebrovascular endothelial cells and it also regulates proliferation, migration, and vessel sprouting.^{11,12} Although the contribution of mitochondria to endothelial cell energy is debated, the evidence supporting its role in cellular signaling has been indisputable.¹³ In cerebral microvasculature, endothelial mitochondria have been shown to regulate the maintenance of BBB.¹⁴ However, to our knowledge, neither cellular energetics nor the relative contribution of OXPHOS and glycolysis were measured in cerebrovascular endothelial cells. Similar to the non-cerebrovascular endothelial cells, glycolysis has been proposed to contribute significantly to ATP generation in the smooth muscle cells (SMC) and regulate their migration and proliferation.^{15,16} OXPHOS was shown to regulate SMC contractility, phenotype switching, and proliferation.^{15,16} Interestingly, recent study has shown that pericytes share glucose and mitochondria with astrocytes and brain microvessels and also promote the survival of astrocytes with impaired energetics by transferring mitochondria.¹⁷ Responses of endothelial cells in the brain are influenced by perivascular cells in the neurovascular unit and characterization of the integrated responses are essential to our understanding of the role of cellular energetics in microvasculature. To date, no study has characterized the microvascular bioenergetics or evaluated the impact of aging on the bioenergetics in BMVs. Our recent technological breakthrough allowed us to measure the oxygen consumption rate (OCR) and extracellular acidification rate (ECAR) from BMVs utilizing the Agilent Seahorse XFe24 analyzer. This technique provides the ability to employ high-throughput assays for quantitative analyses of key pathways contributing to cellular energetics. Considering the unique role of energy metabolism in the cerebral microvasculature, we characterized the glycolytic and OXPHOS pathways of energy generation in the BMVs of young and aged C57Bl/6 mice.

Methods

Materials

Microvessel Isolation. Heparin sodium injection, USP 5000 U/mL (NDC 25021-402-10), Fisherbrand™ FH10 Peristaltic Tubing Pump (13-310-651, Fisher Scientific, Hampton, NH), Butterfly Needle 21 G (135704, Praxisdienst Medical Supplies, Longuich, Germany), Dulbecco's phosphate-buffered saline (DPBS 1X, 14190-144, Gibco, Waltham, MA), Dextran 60–90 kD (180140, MP Biomedicals, Solon, OH), bovine serum albumin fraction V, heat shock (9048-46-8, Roche Diagnostics, Mannheim, Germany), Wheaton 15-mL Tissue grinder (357544, Wheaton, NJ), Centrifuge 5804 R (Eppendorf, Hamburg, Germany), Centrifuge 5430 R (Eppendorf, Hamburg, Germany), non-sterile single-tip cotton swab with wood handle, Falcon™ Cell Strainers 40 µm Nylon (08-771-1, Fisher Scientific, Hampton, NH), pluriStrainer® 300 µm, (43-50300-50, pluriSelect Life Science, Leipzig, Germany), Pierce BCA Protein Assay Kit (23227, Thermo Fisher Scientific, Waltham, MA), NP40 lysis buffer (FNN0021, Invitrogen), protease inhibitor cocktail (P8340, Sigma), phosphatase inhibitor cocktail (P0044, Sigma). **Seahorse Analyzer reagents:** The following reagents were purchased from Agilent Technologies (Santa Clara, CA). XFe24 FluxPak (102340-100), Seahorse XF RPMI media (103576-100), Seahorse XF Real-Time ATP Rate Assay kit (103592-100), Seahorse XF Cell Mito Stress Test kit (103015100), Seahorse XF Glycolytic Rate Assay kit (103344-100), Seahorse XF Mito Fuel Flex Test kit (103260-100). Sodium pyruvate (P8574 Sigma-Aldrich, MO), d-(+)-glucose (G7528, Sigma-Aldrich, MO), GlutaMAX™-I (100X; 35050-061, Gibco, Waltham, MA), Oligomycin complex (11341, Cayman chemicals, Ann Arbor, MI), FCCP (151218, Cayman chemicals, Ann Arbor, MI), Antimycin A (A8674, Sigma-Aldrich, MO), Rotenone (R8875, Sigma-Aldrich, MO). **Enzyme assays:** LDH activity assay kit (ab102526, Abcam), GDH activity (ab102527, Abcam), CS activity (701040, Cayman Chemicals, Ann Arbor, MI).

Animals

All the experiments involving animals were approved by Institutional Animal Care and Use Committee of Tulane University and as per the National Institutes of Health Office of Laboratory Animal Welfare guidelines. We used young (2–4 months-old, purchased from Jackson laboratories) and aged, male C57Bl/6 mice (20–22 months-old, obtained from National Institute on Aging) for this study. The animal data reporting

of the current study has followed the ARRIVE 2.0 guidelines.¹⁸

Brain microvessel isolation

BMVs were isolated as we previously reported.⁹ Briefly mice were anesthetized with isoflurane inhalation and perfused with heparinized phosphate-buffer saline (10 U/ml) for 5 min. Immediately, brains were collected in ice-cold PBS and the cerebral hemispheres were dissected out. Later, cerebral hemispheres were rolled on filter paper to remove the surface vessels and homogenized in PBS. Homogenates were centrifuged at $5000 \times g$ for 15 minutes and the pellet was dissolved in 17.5% dextran solution in PBS. Homogenates were later centrifuged at $7000 \times g$ for 15 minutes, and the pellets were dissolved in the dextran solution to repeat the step. During dextran steps, supernatant along with the floating white matter were carefully taken out with the help of vacuum using glass pipette. Later, supernatants were resuspended in 2% BSA in PBS and filtered through 300 μm filters and the filtrate was later passed through 40 μm filters. The collected microvessels on the 40 μm filters were recovered by washing with 2% BSA solution. Suspension was centrifuged at $7000 \times g$ for 15 minutes and the pellet was resuspended in DMEM and kept on ice until the Seahorse analysis.

Analysis of cellular energetics

We were the first to report a protocol to determine the respiratory function in BMVs.⁹ Briefly, suspensions of BMVs were centrifuged for 10 minutes at $2000 \times g$ at 4°C. DMEM was discarded and the vessel pellet was dissolved in 200 μl seahorse RPMI media. The microvessel preparation was loaded into the cell plate wells. Each well contained BMVs from individual mouse, except for the Mito Fuel Flex Test in which we used pooled microvessels from mice per each well. Cell plates were centrifuged at $2000 \times g$ for 20 minutes at 4°C and kept in a non-CO₂ incubator at 37°C for an hour.

ATP metabolism. The relative contribution of glycolysis and OXPHOS to cellular ATP levels is determined by using a Real-Time ATP Rate Assay. Incubation media contains 25 mM glucose, 10 mM Sodium pyruvate and 2 mM glutamine (pH 7.4). Oligomycin (5 μM) was used in the first injection followed by rotenone/antimycin A (2 $\mu\text{M}/10 \mu\text{M}$). Parameters like glycoATP production rate, mitoATP production rate, and total ATP production rate were measured along with the ATP rate index (mitoATP/glycoATP production rate), percentage of glycolysis, and OXPHOS.

Glycolysis. Glycolytic parameters were measured in the isolated microvessels using a Glycolytic Rate Assay kit. A rotenone and antimycin combination (2 $\mu\text{M}/10 \mu\text{M}$) was used as the first injection followed by 50 mM 2-deoxyglucose (2-DG). Data analysis was performed using the Seahorse Wave Software (Wave 2.6.1, Agilent Technologies, Santa Clara, CA). Parameters including basal glycolysis, induced glycolysis, proton efflux rate (PER), and % PER from glycolysis were measured along with mitoOCR/glycol PER and post 2DG-acidification.

Oxidative phosphorylation. Multiple parameters of mitochondrial function and aerobic cellular respiration were determined with the Cell Mito Stress Test kit. Incubation media contains 25 mM glucose, 10 mM sodium pyruvate and 2 mM glutamate (pH 7.4). Oligomycin (5 μM) was used in the first injection followed by FCCP (5 μM) and rotenone/antimycin A (2 $\mu\text{M}/10 \mu\text{M}$). Parameters like basal respiration, ATP production, maximal respiration, and spare respiratory capacity were measured along with the proton leak and the non-mitochondrial respiration.

Mito fuel flex test. Mitochondrial preference for glucose, glutamine, and fatty acids (FAs) was measured using the Mito Fuel Flex Test kit. Media contains 25 mM glucose, 10 mM Sodium pyruvate and 2 mM glutamine (pH 7.4). Pharmacological inhibitors were used to block the transport of glutamine (3 μM BPTES), FAs (4 μM etomoxir), and glucose (2 μM UK5099) into the mitochondria. The percentage of the preference was reported for the three types of fuels. Seahorse media for all the assays contain 25 mM glucose, 10 mM sodium pyruvate, and 2 mM glutamine (pH 7.4).

Enzyme activities

BMVs from each mouse were digested in 100 μl of NP40 buffer containing protease and phosphatase inhibitors (1:100 dilution), and protein levels were measured using BCA (Thermo Fisher Scientific). Lactate dehydrogenase (LDH), citrate synthase (CS) and glutamate dehydrogenase (GDH) activities were measured in the isolated BMVs from young and aged mice by using the commercially available kits and carried out as per the protocol described by the manufacturer.

LDH activity. Two μl of the tissue homogenate was taken and diluted up to 25 μl with assay buffer and added 25 μl reaction mixture containing the substrate mix in the assay buffer. Absorbance readings were taken at 450 nm for every two minutes for 30 minutes (37°C), to confirm the linear range of the assay. Absorbance values at the zero-time point were deducted from the

absorbance values at the final time point and resulting absorbance values were used to measure the NADH formed using the standard curve. LDH activity was reported as nanomoles of NADH formed/min/ μ g protein.

GDH activity. Three μ l of the tissue homogenate were taken and diluted up to 25 μ l with the assay buffer and added 50 μ l of reaction mixture containing assay buffer, GDH developer and glutamate, and incubated at 37°C. Optical density (OD) readings were taken at 450 nm every 5 minutes for two hours, to confirm the linear range of the assay. Net absorbance values were calculated by deducting zero-hour OD values from two-hour readings. NADH formed was calculated from the standard curve, and the GDH activity was reported as picomoles of NADH formed/min/ μ g protein.

CS activity. Two μ l of the tissue homogenate were diluted up to 15 μ l with the assay buffer, followed by addition of 25 μ l of reagent A and 10 μ l of reagent B. Reagent A contains assay buffer, acetyl CoA reagent and the developer, and reagent B contains oxaloacetate and the buffer. OD readings at 412 nm at 37°C were taken every 2 minutes for 30 minutes. Reaction rates were calculated for every sample, from which the amount of reduced coenzyme formed was measured and reported as nanomoles/min/ μ g protein.

Western blotting

Brain MVs were digested in NP40 lysis buffer containing protease and phosphatase inhibitors by intermittent pipetting on ice. Homogenates were centrifuged (500 \times g for 5 minutes) and the supernatant was used for the immunoblotting. Three-five μ g protein was used for the assays. SDS-PAGE (4–20%) gel electrophoresis and immunoblotting were performed as described previously.¹⁹ Primary antibodies were used at 1:1000 dilution and respective 2nd antibodies were used at 1:5000 dilution. Due to the limited availability of the microvessels samples, we stripped and re-probed the immunoblots to accommodate more protein detection. Proteins include voltage-dependent anion-selective channel 1 (VDAC1, Abcam, ab15895), complex I (NADH:ubiquinone oxidoreductase subunit S4, NDUSF4, Santa Cruz, sc-100567), complex IV (mitochondrially encoded cytochrome c oxidase I, MT-CO1, ab14705), complex II (Succinate Dehydrogenase Complex Flavoprotein Subunit A, SDHA, Santa Cruz, sc-390381), complex III (ubiquinol-cytochrome c reductase complex core protein 2, UQCRC2, sc-390378), complex V (ATP Synthase F1 Subunit Alpha, ATP5A, sc-136178), glucose transporter 1

(GLUT1, Novus Biologicals, NB110-39113), Carnitine Palmitoyl Transferase 1A (CPT1A, NB100-53791), 6-phosphofructo-2-kinase/fructose-2,6-biphosphatase 3 (PFKFB3, Cell Signaling Technology, 13123S), and internal control, β -actin (Sigma, A5441). All the original immunoblots are included in the online supplemental Figures 2 to 17.

Data analysis and statistics

Data analysis for the Mito Stress and Mito Fuel assays was done manually using MS excel, whereas for real-time ATP and glycolytic rates were measured using Seahorse Wave software. Data were reported as the mean \pm SD. Student's t-test was used to calculate the statistical significance between the phenotypes. Appropriate non-parametric test (Mann-Whitney) was used for data that did not follow the normal distribution. $p \leq 0.05$ was taken as the statistical significance. Sample size was calculated based on expected variances and differences between groups from our previous studies.⁹ Age and male sex are used for inclusion and distribution of the animals in the study. Animals were randomly assigned to various assays and the investigators were blinded for data acquisition and analyses purposes. Microvessel isolation, running the assays, western blot and protein/enzyme activity measurements, and data analyses were performed by different laboratory personnel.

Results

Contribution of glycolysis and oxidative phosphorylation to the cellular ATP levels in young and aged brain microvessels

As glycolysis was found to be the major energy provider in various types of endothelial cells, we investigated whether the brain microvessels also use glycolysis as the predominant pathway for ATP production. We used real-time-ATP rate assay and measured the PER and OCR (Figure 1(a) and (b)). Strikingly, majority of the cellular ATP in the young BMVs was found to be generated by OXPHOS compared to glycolysis (11.71 \pm 5.8 vs 5.91 \pm 3.4 pmol ATP/min) (Figure 1(c)). Approximately 70% of the cellular ATP in the young BMVs was generated by OXPHOS and the rest was contributed by glycolysis (67.1 \pm 6.8% vs 32.9 \pm 6.8%) (Figure 1(d)). This was also supported in the young BMVs by the ATP rate index of greater than one which is the ratio of ATP generated from OXPHOS to that of glycolysis (Figure 1(f)). Later, we investigated whether the relative contributions of glycolysis and OXPHOS towards overall ATP production were altered in the BMVs from aged mice. In the

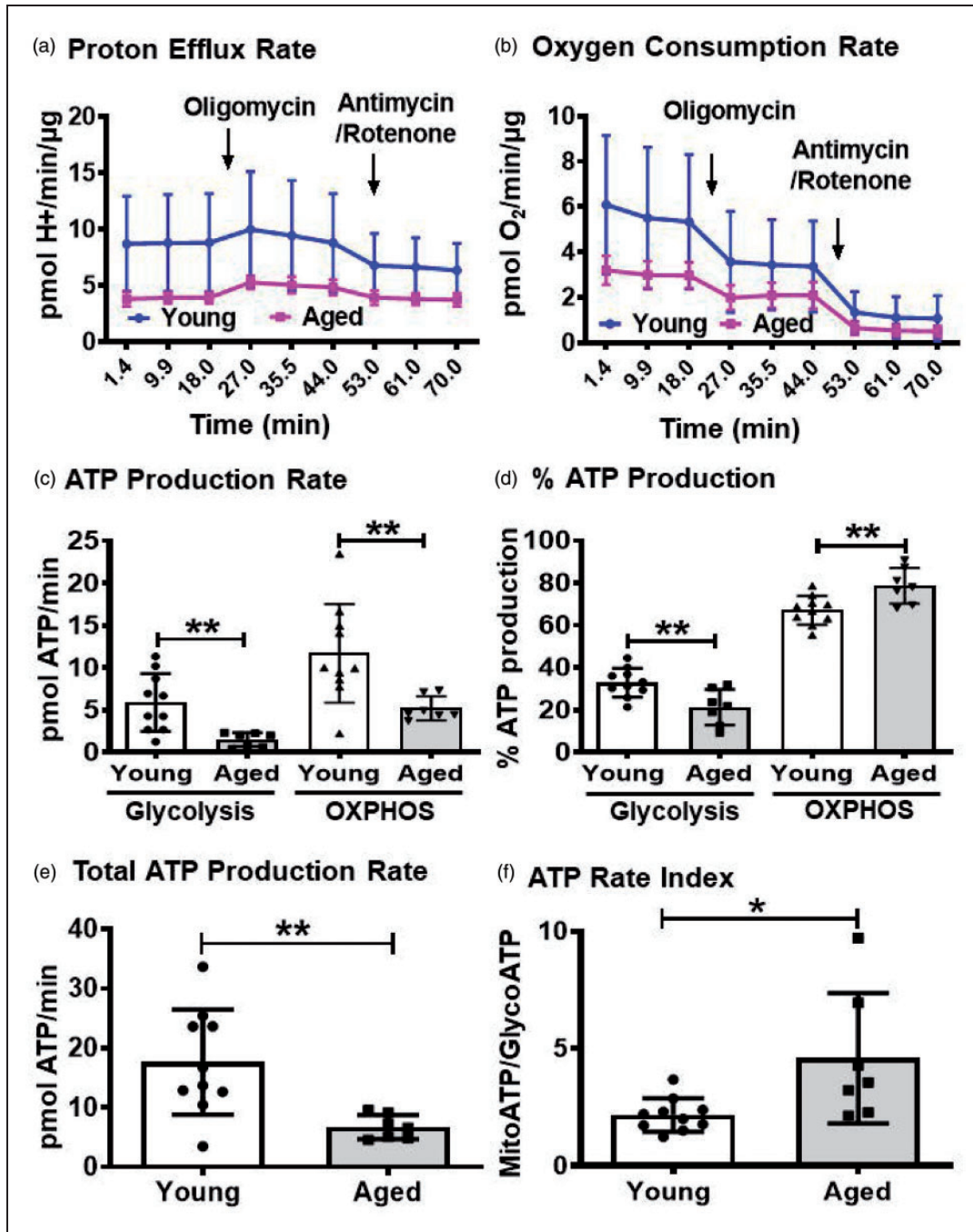


Figure 1. Measuring proton efflux rate, PER (a) and oxygen consumption rate, OCR (b) using Real-time ATP rate assay revealed that OXPHOS is the major contributor for the cellular ATP in the BMVs, and both glycolysis and OXPHOS generation of ATP is impaired with aging (c). Total ATP production is decreased in the aged BMVs (e) and % ATP production (d) and ATP rate Index (f) reveal that despite decreased mitochondrial ATP generation, OXPHOS is the major contributor to the ATP levels in the aged vasculature. PER, proton efflux rate; OCR, oxygen consumption rate (pmol of O₂/min/μg protein). Data were represented as mean ± SD and analyzed by student's t-test. P ≤ 0.05 was taken as the statistical significance. N = 7–10 mice/age group.

aged BMVs, average ATP generated from OXPHOS was decreased by 55.5% (5.20 ± 1.4 vs 11.7 ± 5.82 pmol ATP/min), whereas the contribution from glycolysis towards total ATP generation was found to be significantly decreased by ~74.7% (1.50 ± 0.82 vs

5.91 ± 3.41 pmol ATP/min) (Figure 1(c)). Consistent with these observations, average total ATP production was reduced by 61.8% in the aged BMVs compared to the young BMVs (6.72 ± 2.0 vs 17.6 ± 8.85 pmol ATP/min) (Figure 1(e)). ATP rate index was increased by

112% in the aged BMVs compared to the young BMVs indicating increased contribution of OXPHOS to the cellular ATP in aging (4.58 ± 2.77 vs 2.16 ± 0.71) (Figure 1(f)). Consistent with this, OXPHOS contribution towards ATP is increased by 14.7% (78.71 ± 8.4 vs 67.1 ± 6.8), whereas the glycolysis contribution was decreased by 35% (21.29 ± 8.4 vs 32.9 ± 6.8) in the aged BMVs when compared with the young BMVs (Figure 1(d)).

Glycolytic parameters in the young and aged brain microvessels

Considering the significance of glycolysis in endothelial cells and in other vascular cells, we next measured the

various glycolysis parameters in the young and aged BMVs. Basal glycolysis was reduced significantly by 26.1% (73.9 ± 23.0 vs 100.1 ± 7.7 pmol H^+ /min/ μ g protein) in the aged BMVs compared to that of the younger BMVs (Figure 2(a)). Similarly, compensatory glycolysis decreased by 28.3% (121.0 ± 21.2 vs 168.9 ± 35.5 pmol of H^+ /min/ μ g protein) and the basal proton efflux was reduced by 35.4% (105.2 ± 18.8 vs 162.8 ± 15.8 pmol of H^+ /min/ μ g protein) in the aged BMVs when compared to that of young BMVs (Figure 2(b) and (c)). The percent of PER from glycolysis, mitoOCR/glycoPER ratio, and post-2-DG acidification levels were not different between the young and aged BMVs (Figure 2(d) and (f)) indicating no change in the overall glycolytic phenotype.

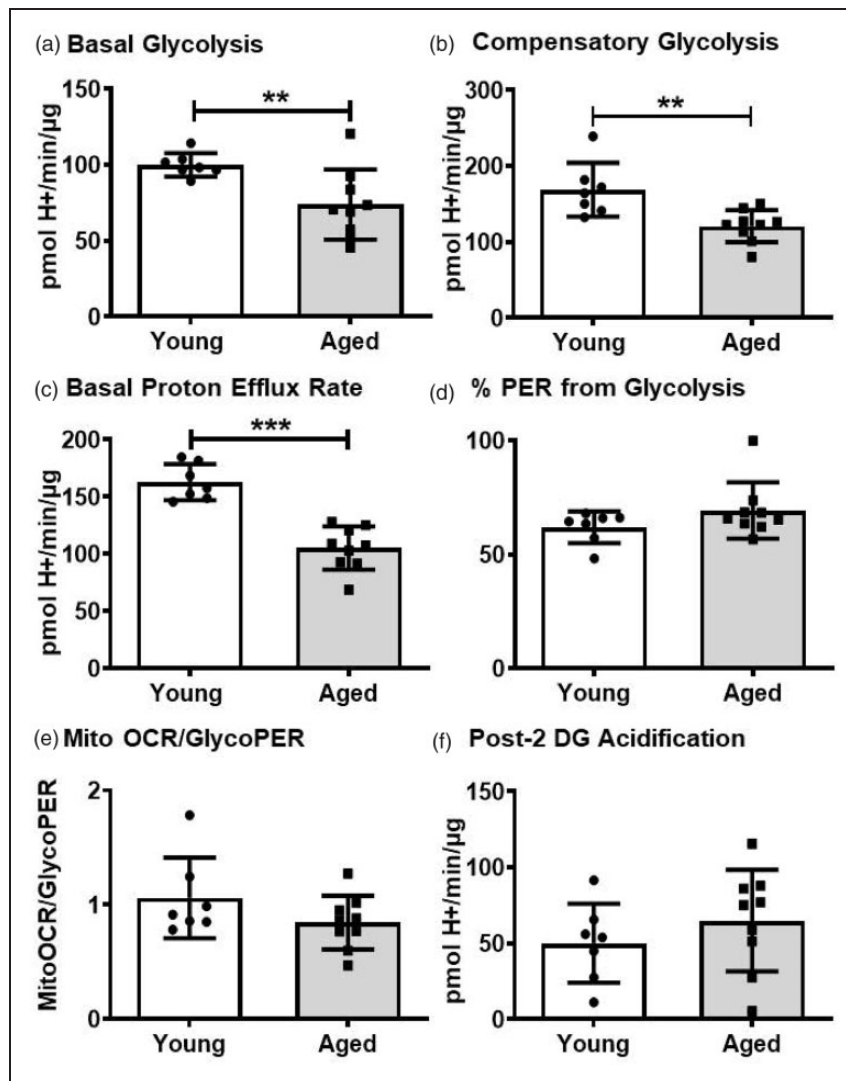


Figure 2. Measuring extracellular acidification rates using glycolytic rate assay revealed that the aged BMVs has compromised basal glycolysis (a), compensatory glycolysis (b), and basal proton efflux rate (PER) (c). % PER from glycolysis (d), glycoPER/Mito OCR (e) and post 2-DG acidification (f) were unaltered between the young and aged BMVs. Data were represented as mean \pm SD and analyzed by student's t-test. $P \leq 0.05$ was taken as the statistical significance. $N = 7-9$ mice/age group.

Post-2DG acidification accounts for the non-glycolytic and mitochondrial TCA-related acidification that includes residual glycolysis not fully inhibited by 2DG and other sources of protons.

To uncover the potential mechanisms underlying the impaired glycolysis in aged BMVs, we measured the protein levels of GLUT1 and PFKFB3 along with LDH activity. GLUT1 is the major transporter of glucose into the endothelial cells and is a critical regulator of brain glucose metabolism. PFKFB3 is a glycolytic enzyme and key regulator of glucose metabolism.

It acts by stimulating the glycolysis through generation of fructose 2, 6-bisphosphate, which is an allosteric activator of phosphofructokinase, a key regulatory enzyme in glycolysis. LDH catalyzes the last step of anaerobic glycolysis, by converting pyruvate to lactate. GLUT1 levels were significantly decreased by 22.5% (0.24 ± 0.10 vs 0.32 ± 0.08) in the aged BMVs when compared to that of the young BMVs (Figure 3(a) and (b)). PFKFB3 levels decreased significantly by 48.5% (0.53 ± 0.22 vs 1.03 ± 0.47) in the aged BMVs when compared to that of the young BMVs (Figure 3

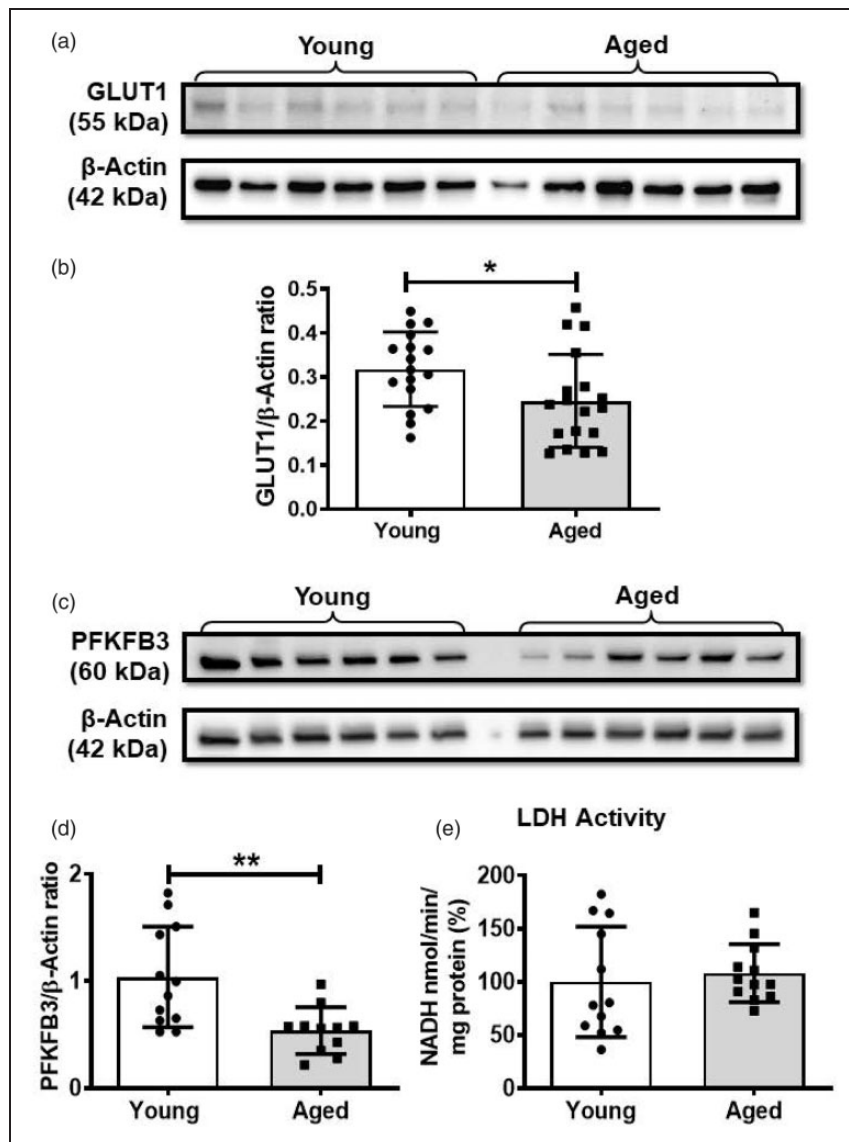


Figure 3. Western blot analysis revealed that the brain microvessels from the aged mice have reduced expression of glucose transporter I (GLUT1) and 6-phosphofructo-2-kinase/fructose-2, 6-biphosphatase 3 (PFKFB3) and unaltered lactate dehydrogenase (LDH) activity. (a). Representative western blot for GLUT1 and internal control, β -actin. (b). GLUT1 to β -actin band density ratio. (c). Western blot for PFKFB3 and internal control, β -actin. (d). PFKFB3 to β -actin band density ratio. (e). LDH activity. Data were represented as mean \pm SD and analyzed by student's t-test. $P \leq 0.05$ was taken as the statistical significance. $N = 17-18$ mice/age group (GLUT1 expression and LDH activity), $N = 12$ mice/age group (PFKFB3 expression). All the original immunoblots are included in the online supplementary figures (2-5).

(c) and (d)). LDH activity was not altered with the aging in the BMVs (Figure 3(e)).

Mitochondrial respiratory parameters in the young and aged brain microvessels

As we observed a more significant role of OXPHOS towards energy metabolism in BMVs in contrast to the previous observations in the endothelial cells²⁰

and because functional mitochondria are critical in the cell signaling, we measured the mitochondrial respiration in the isolated BMVs from the young and the aged mice. Basal respiration was decreased significantly by 21.2% (81.5 ± 24.4 vs 103.4 ± 19.6 pmol of O_2 /min/ μ g protein) in the BMVs from aged mice compared to the young mice (Figure 4(a)). ATP production was unaltered between the young and aged BMVs, whereas the maximal respiration was decreased by 23.7%

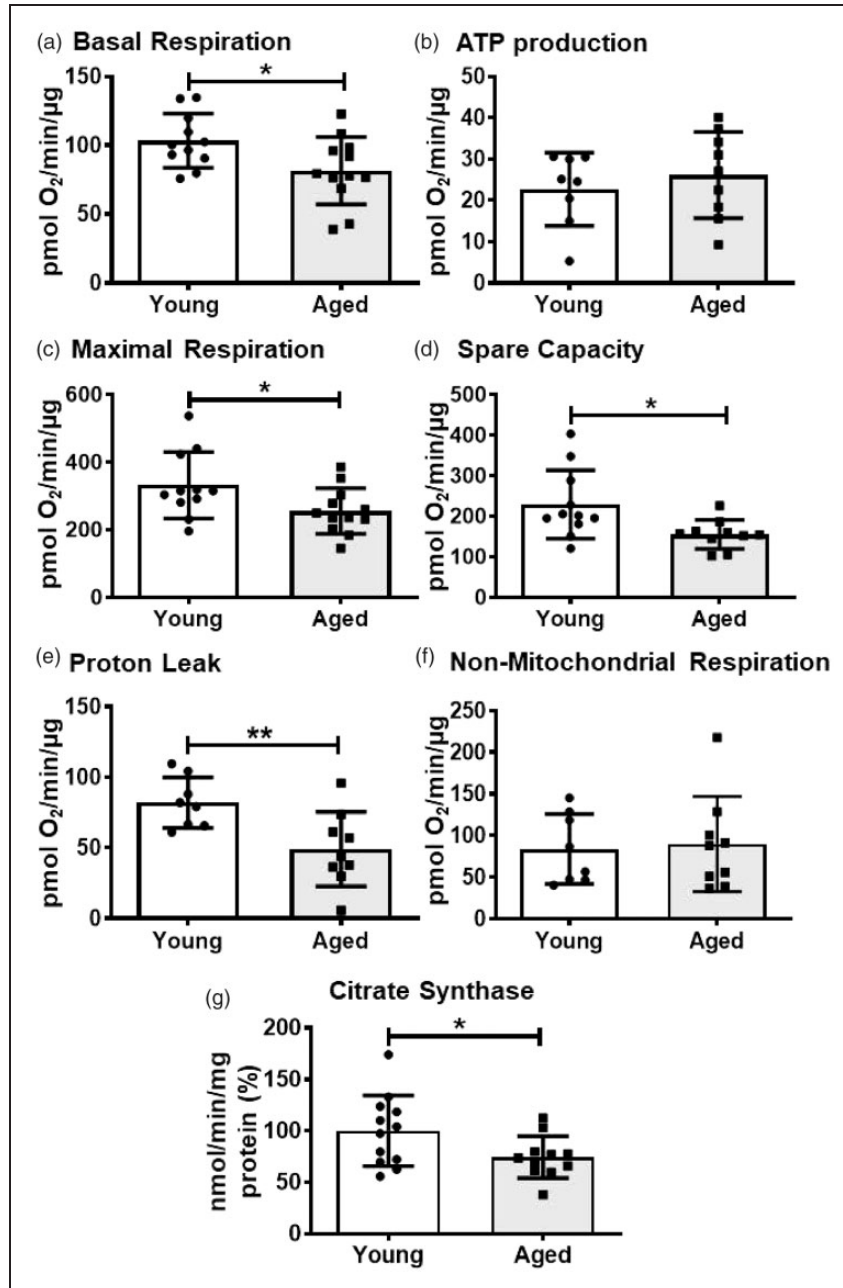


Figure 4. Measuring oxygen consumption rate (OCR) using Mito stress assay revealed that aged BMVs have impaired mitochondrial respiration and citrate synthase activity. (a) Basal Respiration. (b) ATP production. (c) Maximal respiration. (d) Spare capacity. (e) Proton leak. (f) Non-mitochondrial respiration. (g) Citrate synthase activity. Data were represented as mean \pm SD and analyzed by student's t-test. $P \leq 0.05$ was taken as the statistical significance. $N = 8-12$ mice/age group.

(255.4 ± 67.7 vs 332.3 ± 98.3 pmol of O_2 /min/ μ g protein) and respiratory spare capacity by 32.2% (155.1 ± 35.7 vs 228.9 ± 84.7 pmol of O_2 /min/ μ g protein) in the aged BMVs when compared with the BMVs from the young mice (Figure 4(b) to (d)). Interestingly, proton leak was decreased significantly by 40.3% (48.95 ± 26.4 vs 81.9 ± 17.9 pmol of O_2 /min/ μ g protein) in the aged BMVs when compared with the young BMVs (Figure 4(e)). Non-mitochondrial respiration was not altered between the two age groups (Figure 4(f)).

To understand the possible mechanisms involved in the decreased mitochondrial respiration in the aged BMVs, we measured the activity of citrate synthase, a key regulatory enzyme of TCA cycle along with expression of ETC complex proteins and VDAC, a key transporter of adenine nucleotides and Ca^{2+} into the mitochondria. Activity of CS enzyme was decreased significantly by 25.7% (74.3 ± 20.3 vs 100 ± 34.5 nmol/min/ μ g protein) in the aged BMVs when compared to that of the young BMVs (Figure 4(g)). The protein levels of VDAC and of subunits of complex II, IV and ATP synthase were not altered in the aged BMVs (Figure 5).

Mitochondrial fuel preferences in the young and aged brain microvessels

As mitochondria can utilize various substrates including glucose, glutamine, and FAs as the fuel for ATP production, we measured the mitochondrial fuel preference in the BMVs followed by a comparison between the two age groups. Glucose is the most preferred fuel ($43.4 \pm 5.0\%$) by the mitochondria of the BMVs followed by equal preferences for glutamine ($26.7 \pm 3.7\%$) and FAs ($29.9 \pm 2.1\%$) (Figure 6(a)). Mitochondrial preference towards glucose showed a decreasing trend (37.7 ± 2.4 vs $43.4 \pm 5.0\%$, $p = 0.13$) in the aged BMVs compared with the young BMVs (Figure 6(a)). Interestingly, mitochondrial utilization of glutamine towards OXPHOS was increased by 22.2% in the aged BMVs when compared with the young BMVs (32.67 ± 1.2 vs 26.7 ± 3.7) (Figure 6(a)). Mitochondrial preference for FAs was unaltered in the aged BMVs (Figure 6(a)).

To understand the mechanism involved in the increased utilization of glutamine by mitochondria of the aged BMVs, we measured the activity of GDH, an enzyme that converts glutamate to α -ketoglutarate (α -KG), an intermediate of the TCA cycle. GDH activity is significantly increased by 19.8% (116.8 ± 15.0 vs 93.6 ± 24.1 pmol of NADH/min/ μ g protein %) in the aged BMVs when compared to the young BMVs (Figure 6(b)).

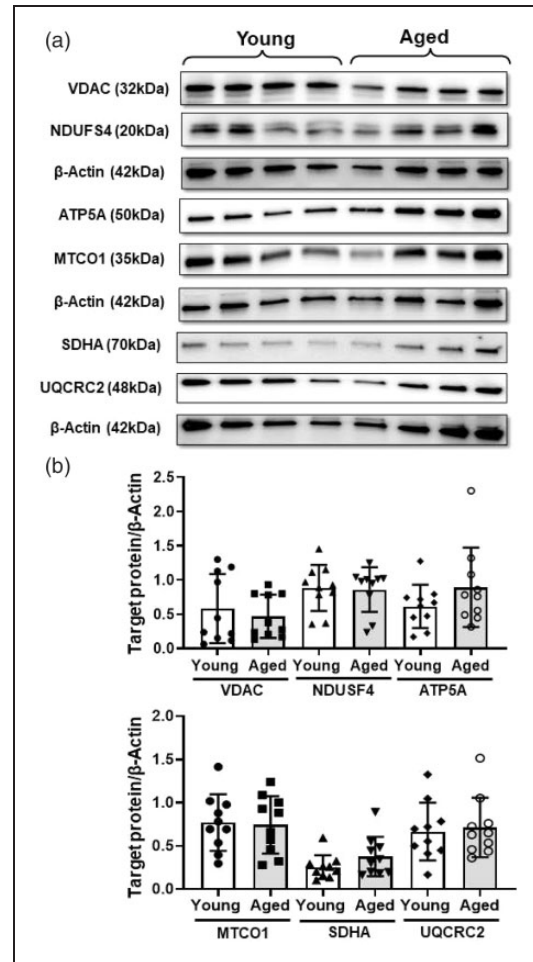


Figure 5. Western blot analysis revealed unaltered mitochondrial voltage-dependent anion channel (VDAC) and electron transport chain (ETC) complex proteins. (a) Representative western blot images of VDAC, complex I ((NADH:ubiquinone oxidoreductase subunit S4, NDUF54, Santa Cruz, sc-100567), complex V (ATP Synthase F1 Subunit Alpha, ATP5A), complex IV (mitochondrially encoded cytochrome c oxidase I, MT-CO1), complex II (Succinate Dehydrogenase Complex Flavoprotein Subunit A, SDHA), complex III (ubiquinol-cytochrome c reductase complex core protein 2, UQCRC2), and β -actin as internal control. (b). Cumulative data of the immunoband intensity are represented as bar graphs of respective protein to β -actin band density ratios. Data were represented as mean \pm SD and analyzed by student's t-test. $P \leq 0.05$ was taken as the statistical significance. $N = 10$ mice/age group. All the original immunoblots are included in the online supplementary Figures 6 to 14.

Though we did not observe the changes in the FA oxidation, we measured the proteins levels of mitochondrial FA transporter, CPT1A, using western blotting. Levels of CPT1A were not different between the two age groups consistent with the OCR measurements (Figure 6(c)). Notably, CPT1B and CPT2 isoforms

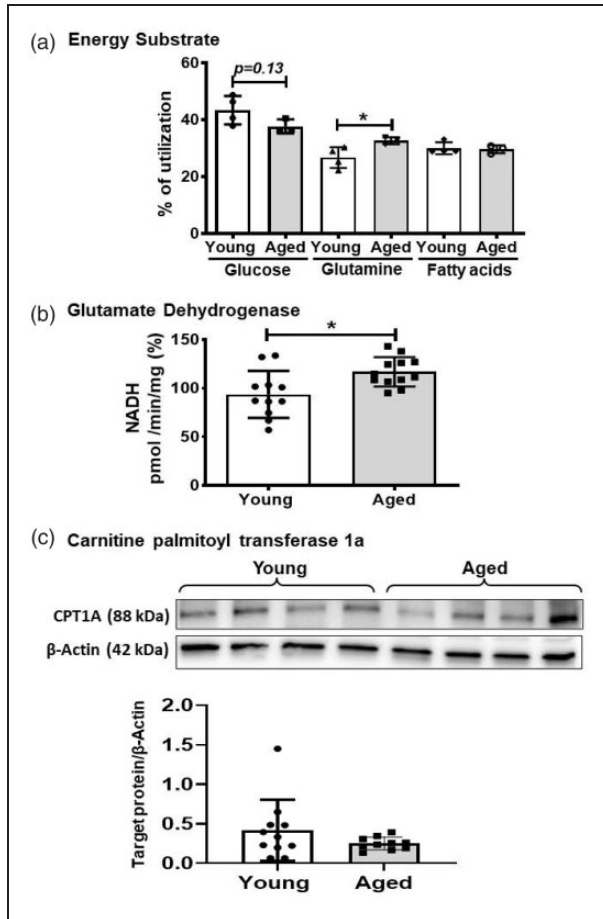


Figure 6. Measuring OCR using Mito fuel assay revealed that mitochondria from the aged BMVs utilize more glutamate for oxidative phosphorylation. (a). % of utilization of metabolic fuels by cerebral microvascular mitochondria. (b). Glutamate dehydrogenase (GDH) activity. (c). Representative western blots and bar graph for carnitine palmitoyltransferase 1a (CPT1a) and β -actin proteins and their density ratio. Data were represented as mean \pm SD and analyzed by student's t-test. $P \leq 0.05$ was taken as the statistical significance. $N = 4$ (pooled from 12 mice) for young mice and $N = 3$ (pooled from 9 mice) for aged mice. $N = 11$ –12 mice for GDH activity, and $N = 10$ mice for CPT1a westerns. All the original immunoblots are included in the online supplementary figures (15–16).

were not detectable in the BMVs (supplementary Figures 15 and 16)).

Discussion

The present study for the first time characterized the energetics of freshly isolated brain microvessels *ex vivo* and identified the impact of aging on the energy pathways. The study is significant to demonstrate distinctly different metabolic characteristics of BMVs versus the previously reported energy phenotype of endothelial cells from other vascular beds.^{12,21,22} We employed

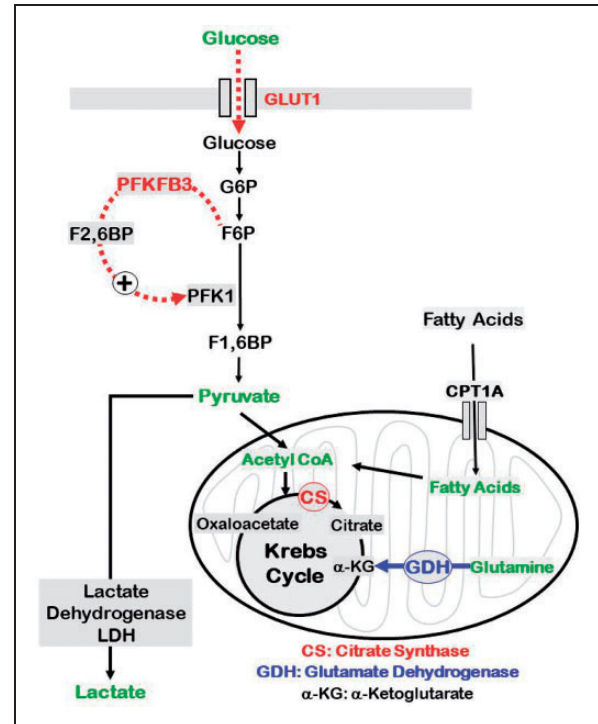


Figure 7. Schematic of key impairments in the energy metabolism in aged BMVs. Impairments of glucose metabolism in aged BMVs involve decreased expression of GLUT1 and PFKFB3. GLUT1 is the primary transporter of glucose whereas PFKFB3 is a key activator of pyruvate generation in the glycolytic pathway. Interestingly, metabolism of pyruvate by lactate dehydrogenase (LDH) into lactate, the critical step in the anaerobic respiration, was not altered in aged BMVs under the conditions of our study. On the other hand, metabolism of acetyl coenzyme A (CoA) into citrate by citrate synthase (CS) was reduced in aged BMVs. Formation of citrate from acetyl CoA is the first step in the Krebs cycle and reduced activity of CS thus could contribute to impaired OXPHOS in aged BMVs by reducing generation of electron donors ($FADH_2$ and NADH). Notably, despite the above biochemical impairments in energy pathways, utilization of glucose or FAs were affected in aged BMVs. Interestingly, utilization of glutamine was found to be increased in aged BMVs. Consistent with this, we observed increased activity of GDH that catalyzes the conversion of α -KG from glutamine. α -KG is an intermediate in the Krebs cycle, increased flux of which could maintain the Krebs cycle activity in the presence of decreased CS activity. Thus, we identified several biochemical mechanisms contributing to the impaired energetics in aged BMVs that also include compensatory mechanisms. Enzymes/proteins highlighted in red indicate down regulation and highlighted in blue indicate upregulation in aged mice.

BMVs in the study that predominantly contain capillaries as we^{6,7,9} and others⁸ have previously demonstrated. The major findings of the study as summarized in Figure 7 are: first, unlike the endothelial cells from other vascular beds,^{12,21,22} BMVs, predominantly containing endothelial cells, depended on OXPHOS/mitochondria for ATP generation. Second, aging

induced reduction of total ATP generation in BMVs by impairing both OXPHOS and glycolysis. Third, aging induced impairments of OXPHOS involved diminished spare respiratory capacity with no alteration in the ETC complex protein levels. Fourth, aging induced reduction of glycolysis involved reduced compensatory glycolysis that was accompanied by reduced protein levels of glucose transporter (GLUT1) and the key activator of glycolysis (PFKFB3). Finally, aging induced compensatory increase in utilization of glutamine as fuel substrate by BMVs. Thus, the impairments of both the energy pathways deprive the aged BMVs of the energy safeguards afforded by nature and make them vulnerable to injury when they are exposed to energy crises such as ischemia-reperfusion (IR) injury, diabetes, or β -amyloid toxicity.

Endothelial cells have been proposed to be dependent primarily on glycolysis for energy needs as studies have reported that more than 85% of cellular ATP is derived from glycolysis.^{12,22,23} Non-reliance on OXPHOS for energy production is proposed to be advantageous as relying on glycolysis spares the oxygen for perivascular cells¹² and protects against mitochondrial superoxide generation. To date, endothelial mitochondria in peripheral vascular beds are considered to be important primarily for cellular signaling but not as a significant source of cellular ATP.¹² Moreover, lower mitochondrial numbers of 2–6% of cytoplasmic volume in endothelial cells is attributed to their insignificant role in energetics.²⁴ Interestingly, brain microvascular endothelial cells were reported to contain greater number of mitochondria, occupying 8–11% of the cytoplasmic volume that is critical for maintaining various energy consuming transport processes across the BBB.^{12,25} However, the contribution of mitochondria to cellular energy in the BMVs has never been studied. Recent studies in HUVECs found that mitochondrial respiration is essential for endothelial cell homeostasis, proliferation, and angiogenesis.^{26,27} Interestingly, during angiogenesis, tip cells were shown to be less glycolytic and more OXPHOS dependent.^{12,27} Similarly, mitochondrial respiratory defects have been shown to mediate stroke-induced BBB leakage, indicating that mitochondrial OXPHOS is critical in microvascular function.¹⁴ To date, there have been no reports characterizing the glycolysis and OXPHOS in the cerebral microvasculature. Contrary to the previous observations in endothelial cells, our study for the first time revealed that OXPHOS is the dominant energy source in BMVs contributing to ~70% of the total ATP. It is noted that studies of energetics in endothelial cells to date have employed mostly cells from umbilical vein, coronary microvasculature, and aorta that derive energy from glycolysis. Greater dependence on OXPHOS by the BMVs may

be logical as they have high energy demand and OXPHOS provides more ATP per mole of glucose. Also, neurons are solely dependent on glucose, therefore relying on high-glucose consuming glycolysis by BMVs decreases glucose availability to neuronal tissue.

Aging is associated with endothelial dysfunction leading to impaired BBB function, neurovascular coupling, and impaired angiogenesis after the stroke.^{3,4,28,29} Mitochondrial respiratory defects have been shown to induce senescence in endothelial cells.^{14,27,30} Interestingly, we found that various mitochondrial respiratory parameters were decreased in the BMVs of aged mice. The elevated ATP rate index indicates that, despite the mitochondrial impairments, aged BMVs continued to rely more on OXPHOS as the predominant source for ATP generation than on glycolysis. It is noted that energy pathways act as mutual backups and reductions in mitochondrial respiratory function are expected to be compensated by upregulation of glycolytic energy generation or initiating metabolic switching.³¹ However, we found that aged BMVs also display diminished glycolytic ATP production compared to young BMVs. Evidence indicates that the relationship between glycolysis and aging brain is complex due to the cell-specific differential alterations of glycolysis.^{32–34} Aged BMVs showed reduced compensatory glycolysis, a measure of the ability of the cells to compensate for loss of ATP generation under conditions of mitochondrial inhibition/damage. Thus, diminished compensatory glycolysis in aged BMVs make them more vulnerable to hypoxic or IR injury.

In order to validate the functional evidence from OCR and ECAR measurements in BMVs, we determined the protein levels and activity of key regulators of energy metabolism. Insulin-sensitive GLUT1 is the major glucose transporter in the cerebral endothelial cells and transports the glucose to the brain tissues from the systemic circulation.^{35,36} GLUT1, but not the neuronal GLUT3, is considered to be primarily responsible for neuronal glucose metabolism and neurometabolic coupling.^{36–38} Subjects with the genetic disorder, GLUT1 deficiency syndrome, display low cerebrospinal fluid, seizures, and developmental delay, further indicating the importance of GLUT1 in cerebral metabolism.³⁹ GLUT1 expression has been shown to be decreased in ischemia and AD.^{40,41} Endothelial GLUT1 deficiency has been found to be associated with BBB breakdown, cerebrovascular degeneration, diminished blood flow, and impaired cognition.^{41,42} Interestingly, aging has been shown to decrease GLUT1 expression in endothelial cells.⁴³ To our knowledge, GLUT1 expression was not reported in the aged BMVs or the cerebral endothelial cells. For the first time, we observed decreased GLUT1 levels in the aged BMVs that is likely to have contributed to the

diminished OXPHOS and the glycolysis. Furthermore, hypoxia-inducible factor-1 α , an important mediator of cellular response to hypoxia was found to be essential for transendothelial glucose transport into brain through regulation of GLUT1 expression.³⁶ It was well documented that HIF-1 α signaling is decreased in the aged endothelial cells leading to impaired vascular responses to ischemia.⁴⁴ Thus, aging induced reduction of GLUT1 levels may likely contribute to the vulnerability to hypoxic/ischemic injury. In glycolytic flux, phosphofructo-1 kinase (PFK-1), which catalyzes one of the three rate-limiting checkpoints, is activated by fructose-2, 6-bisphosphate (F2,6P₂). In endothelial cells, F2,6P₂ is synthesized by PFKFB3. PFKFB3-driven glycolysis makes endothelial cells to be sensitive to laminar shear stress⁴⁵ and has been implicated in vessel sprouting.²² Inhibition or deletion of PFKFB3 disrupts angiogenesis.^{20,46} Moreover, reduced PFKFB3-driven glycolysis has been shown to promote microvascular rarefaction.⁴⁷ Our studies for the first time observed diminished levels of PFKFB3 in aged BMVs that could contribute to reduced glycolysis. Although inhibition of PFKFB3 has been shown to be neuroprotective against experimental stroke,⁴⁸ microvascular rarefaction accompanying reduced PFKFB3 activity may promote age-related vulnerability to ischemic brain injury. Interestingly, aged BMVs display unchanged LDH activity compared to young BMVs indicating that diminished activity of upstream regulators promotes aging-associated reduced glycolytic rate. It is noted that the evidence of angiogenesis has been reported in humans and animals after ischemic brain injury.⁴⁹ However, the therapeutic benefit or aggravating stroke progression of post-stroke angiogenesis have been intensely debated.⁴⁹ It has been proposed that formation of mature and functional blood vessels, a major failure in the majority of angiogenesis-based therapies, require recruitment of pericytes.⁴⁹ The BMVs employed in the present study contain pericytes (Supplementary Figure 1) although endothelial cells are the predominant cell type. Thus, endothelial cells and pericytes in the BMVs could collectively contribute to the glycolytic pathway impairments that are detrimental to the neurorestorative post-stroke angiogenesis in aged mice.

As we have previously reported,⁹ aged BMVs displayed reduced basal and maximal respiration compared to young BMVs. It is noted that OCR values linked to the ATP production obtained from Cell Mito Stress Test were unchanged in the aged BMVs. In contrast, total, glycolytic and OXPHOS linked ATP production rates calculated by the XF Report Generator software from Real Time ATP Rate assay data were reduced in aged BMVs. To convert ATP-coupled OCR into mitochondrial ATP

Production Rate, a theoretical value representing the stoichiometry of ATP phosphorylated per atoms of oxygen reduced (P/O ratio) is incorporated into the calculations. Thus, the latter calculations considering the stoichiometry of each metabolic fuel combined with experimental results obtained using isolated mitochondria and considering F₁F₀-ATP synthase efficiency provide accurate estimates of cellular ATP production. Furthermore, aged BMVs exhibit diminished spare respiratory capacity compared to the young BMVs indicating their inability to enhance electron transport or OCR under conditions that require maintaining proton motive force when faced with uncoupling or to generate excess ATP. Similarly, aged BMVs also displayed reduced proton leak compared to young BMVs. Activation of proton leak, presumably through uncoupling protein (UCP) channels in the inner mitochondrial membrane, prevents the overcharging of the inner mitochondrial membrane potential thereby reducing the mitochondrial superoxide generation. Thus, reduced proton leak in aged BMVs may likely promote mitochondrial oxidative stress.³¹ Incidentally, we have not been able to reliably identify any UCPs in the BMVs despite our best efforts with multiple antibodies (data not shown), this may be due to low levels of protein.

The decreased mitochondrial respiration in the aged BMVs may be due to decreased mitochondrial numbers, or downregulation of ETC proteins/function or reduced substrate availability and metabolism. Previous studies reported a decrease in the mitochondrial numbers in the aged capillary endothelial cells.⁵⁰ Aging related alterations of Krebs cycle enzyme activities,⁵¹ including CS activity⁵² as well as ETC proteins⁵³ and nicotinamide adenine dinucleotide (NAD⁺)^{54,55} levels, have been previously reported in the brain mitochondria. We found diminished CS activity in the aged BMVs for the first time. CS activity is widely used as the mitochondrial mass marker, however, our immunoblots observed that protein levels of ETC complexes and VDAC in BMVs were unaffected by aging. Thus, it is likely that reduced CS activity is independent of mitochondrial mass in aged BMVs. Reduced CS activity could reduce the metabolism of pyruvate through Krebs cycle and generation of electron donors/substrates for ETC thereby contributing to diminished mitochondrial respiratory parameters.

The Mito Fuel Flex Test has demonstrated that glucose remains the predominant energy substrate in young BMVs, followed by equal contribution from FAs and glutamine. The relative contribution of FA and glutamine to energy production in endothelial cells have been shown to be essential for vessel sprouting.^{11,12,23} Notably, aged BMVs showed increase in glutamine utilization for ATP generation compared

to young BMVs. Glutamine is the most abundant amino acid in extracellular compartment whereas glutamate is the most abundant amino acid in the intracellular compartment.⁵⁶ Glutamine enters the TCA cycle through two enzymatic conversions. Initial glutamine conversion to glutamate is catalyzed by glutaminases and subsequent glutamate conversion to α -KG is catalyzed by GDH. Recent studies have reported GDH activity in the cerebral capillaries and endothelial cells.⁵⁷ Interestingly, metabolism of glutamate through OXPHOS was found to be increased in the absence of glucose in the brain endothelial cells.⁵⁷ In mammalian cells with impaired mitochondrial respiration resulting from mitochondrial DNA mutations, elevated glutamine metabolism was found to be critical for energy production and for anaplerosis.⁵⁸ Supporting our respiration measurements, we found that the activity of GDH was increased in aged BMVs. Similar increase in GDH activity was also previously reported in aged brain mitochondria.⁵⁹ It is noted that α -KG is not only an intermediate in Krebs cycle but also a substrate for demethylases that modify both protein and DNA. Thus, increase in GDH activity in aged BMVs attempts to compensate for other impairments in Krebs cycle enzymes as well as ETC components albeit with modest results. In contrast, consistent with respiratory measurements, fatty acid transport into mitochondria was not found to be affected in aged BMVs reflected by the unchanged CPT1A levels in BMVs from aged compared with BMVs from young mice.

Limitations

The BMVs used in the study contain capillaries, venules, and precapillary arterioles with majority of them being capillaries as we^{6,7,9} and others⁸ have previously demonstrated. Although the BMVs are heterogeneous in cellular composition, more than 90% of them are capillaries. However, we have found that the capillaries also contain pericytes (supplementary Figure 1) although endothelial cells significantly outnumbered pericytes. Thus, the bioenergetics we measured reflect predominantly cerebral microvascular endothelial cells with contribution from pericytes. The value of employing BMVs is twofold: first, to our knowledge, there have been no previous reports of cellular energetics in cerebral microvasculature. Second, majority of the reports of bioenergetics of endothelial cells employed cultured cells but not freshly isolated cells as in the present study. Future studies are needed to evaluate the age-related alterations in energy phenotype of endothelial cells and pericytes independent of each other. Although young (Jackson Laboratories) and aged (National Institute of Aging) mice were obtained from two different sources, the founder line (C57Bl6)

remained the same. There were no studies comparing the differences in aging and our proteomics data supported the functional data in the present study. Lastly, our study did not include female mice and future studies will address the potential sex-dependent differences in bioenergetics of BMVs and microvascular aging.

In conclusion, the alterations of cellular energetics, protein expression, and enzyme activities in aged BMVs taken together indicate that the substrate availability and metabolism were impaired in the aged BMVs leading to decreased ATP production. Despite a modest increase glutamine utilization, multiple impairments in the OXPHOS and glycolytic pathways in aged BMVs make them vulnerable to injury under conditions of high energy demand and/or mitochondrial damage such as stroke, diabetes, or β -amyloid toxicity.

Funding

The author(s) disclosed receipt of the following financial support for the research, authorship, and/or publication of this article: This research project was supported by the National Institutes of Health: National Institute of Neurological Disorders and Stroke (NS094834 and NS114286 – P.V. Katakam; NS114286 – R. Mostany; NS096237 – D. Atochin), National Institute on Aging (AG074489 – P.V. Katakam and R. Mostany; AG047296 – R. Mostany; R01AG049821 – W.L. Murfee), and National Institute of General Medical Sciences (NS094834 - P.V. Katakam). In addition, the study was supported by American Heart Association (National Center Scientist Development Grant, 14SDG20490359 - P.V. Katakam; Greater Southeast Affiliate Predoctoral Fellowship Award, 16PRE27790122 - V.N. Sure; Predoctoral Fellowship Award, 20PRE35211153 - W.R. Evans. The content is solely the responsibility of the authors and does not necessarily represent the official views of the National Institutes of Health.

Acknowledgments

We thank Ms. Sufen Zheng for her technical help for the studies.

Declaration of conflicting interests


The author(s) declared no potential conflicts of interest with respect to the research, authorship, and/or publication of this article.

Authors' contributions

R.M., W.L.M., D.N.A., and P.V.K. conceived and designed the experiments; S.S.V.P., V.N.S., L.K., W.R.E., J.A.S., and P.V.K. performed experiments; S.S.V.P., V.N.S., L.K., R.M., and P.V.K. analyzed data; S.S.V.P., D.N.A., W.L.M., R.M., and P.V.K. interpreted experimental results, and prepared figures; S.S.V.P., R.M., and P.V.K. drafted the manuscript; S.S.V.P., V.N.S., L.K., W.R.E., J.A.S., G.J.B., X.W., W.L.M., R.M., and P.

V.K. edited and revised the manuscript and approved the final version of the manuscript.

ORCID iD

Prasad VG Katakam  <https://orcid.org/0000-0002-4708-9140>

Supplemental material

Supplemental material for this article is available online.

References

- Benjamin EJ, Muntner P, Alonso A, et al.; American Heart Association Council on Epidemiology and Prevention Statistics Committee and Stroke Statistics Subcommittee. Heart disease and stroke statistics-2019 update: a report from the American Heart Association. *Circulation* 2019; 139: e56–e528.
- Hicks P, Rolsten C, Brizzee D, et al. Age-related changes in rat brain capillaries. *Neurobiol Aging* 1983; 4: 69–75.
- Erdő F, Denes L and de Lange E. Age-associated physiological and pathological changes at the blood-brain barrier: a review. *J Cereb Blood Flow Metab* 2017; 37: 4–24.
- Toth P, Tarantini S, Csiszar A, et al. Functional vascular contributions to cognitive impairment and dementia: mechanisms and consequences of cerebral autoregulatory dysfunction, endothelial impairment, and neurovascular uncoupling in aging. *Am J Physiol Heart Circ Physiol* 2017; 312: H1–h20.
- Chen MB, Yang AC, Yousef H, et al. Brain endothelial cells are exquisite sensors of Age-Related circulatory cues. *Cell Rep* 2020; 30: 4418–4432.e4. 414.
- Cikic S, Chandra PK, Harman JC, et al. Sexual differences in mitochondrial and related proteins in rat cerebral microvessels: a proteomic approach. *J Cereb Blood Flow Metab* 2021; 41: 397–412.
- Chandra PK, Cikic S, Baddoo MC, et al. Transcriptome analysis reveals sexual disparities in gene expression in rat brain microvessels. *J Cereb Blood Flow Metab* 2021; 41: 2311–2328.
- Lee YK, Uchida H, Smith H, et al. The isolation and molecular characterization of cerebral microvessels. *Nat Protoc* 2019; 14: 3059–3081.
- Sure VN, Sakamuri S, Sperling JA, et al. A novel high-throughput assay for respiration in isolated brain microvessels reveals impaired mitochondrial function in the aged mice. *Geroscience* 2018; 40: 365–375.
- Chaitanya GV, Minagar A and Alexander JS. Neuronal and astrocytic interactions modulate brain endothelial properties during metabolic stresses of in vitro cerebral ischemia. *Cell Commun Signal* 2014; 12: 7.
- Eelen G, Cruys B, Welti J, et al. Control of vessel sprouting by genetic and metabolic determinants. *Trends Endocrinol Metab* 2013; 24: 589–596.
- Eelen G, de Zeeuw P, Treps L, et al. Endothelial cell metabolism. *Physiol Rev* 2018; 98: 3–58.
- Caja S and Enríquez JA. Mitochondria in endothelial cells: sensors and integrators of environmental cues. *Redox Biol* 2017; 12: 821–827.
- Doll DN, Hu H, Sun J, et al. Mitochondrial crisis in cerebrovascular endothelial cells opens the blood-brain barrier. *Stroke* 2015; 46: 1681–1689.
- Chiong M, Cartes-Saavedra B, Norambuena-Soto I, et al. Mitochondrial metabolism and the control of vascular smooth muscle cell proliferation. *Front Cell Dev Biol* 2014; 2: 72.
- Narayanan D, Xi Q, Pfeffer LM, et al. Mitochondria control functional CaV1.2 expression in smooth muscle cells of cerebral arteries. *Circ Res* 2010; 107: 631–641.
- Castro V, Skowronska M, Lombardi J, et al. Occludin regulates glucose uptake and ATP production in pericytes by influencing AMP-activated protein kinase activity. *J Cereb Blood Flow Metab* 2018; 38: 317–332.
- Percie Du Sert N, Hurst V, Ahluwalia A, et al. The ARRIVE guidelines 2.0: updated guidelines for reporting animal research. *J Cereb Blood Flow Metab* 2020; 40: 1769–1777.
- Albuck AL, Sakamuri S, Sperling JA, et al. Peroxynitrite decomposition catalyst enhances respiratory function in isolated brain mitochondria. *Am J Physiol Heart Circ Physiol* 2021; 320: H630–H641.
- Li X, Sun X and Carmeliet P. Hallmarks of endothelial cell metabolism in health and disease. *Cell Metab* 2019; 30: 414–433.
- De Bock K, Georgiadou M and Carmeliet P. Role of endothelial cell metabolism in vessel sprouting. *Cell Metab* 2013; 18: 634–647.
- De Bock K, Georgiadou M, Schoors S, et al. Role of PFKFB3-driven glycolysis in vessel sprouting. *Cell* 2013; 154: 651–663.
- Kalucka J, Ghesquiere B, Fendt SM, et al. Analysis of endothelial fatty acid metabolism using tracer metabolomics. *Methods Mol Biol* 2019; 1978: 259–268.
- Kluge MA, Fetterman JL and Vita JA. Mitochondria and endothelial function. *Circ Res* 2013; 112: 1171–1188.
- Oldendorf WH, Cornford ME and Brown WJ. The large apparent work capability of the blood-brain barrier: a study of the mitochondrial content of capillary endothelial cells in brain and other tissues of the rat. *Ann Neurol* 1977; 1: 409–417.
- Yetkin-Arik B, Vogels IMC, Nowak-Sliwinska P, et al. The role of glycolysis and mitochondrial respiration in the formation and functioning of endothelial tip cells during angiogenesis. *Sci Rep* 2019; 9: 12608.
- Yetkin-Arik B, Vogels IMC, Neyazi N, et al. Endothelial tip cells in vitro are less glycolytic and have a more flexible response to metabolic stress than non-tip cells. *Sci Rep* 2019; 9: 10414.
- Graves SI and Baker DJ. Implicating endothelial cell senescence to dysfunction in the ageing and diseased brain. *Basic Clin Pharmacol Toxicol* 2020; 127: 102–110.
- Petcu EB, Smith RA, Miroiu RI, et al. Angiogenesis in old-aged subjects after ischemic stroke: a cautionary note for investigators. *J Angiogenesis Res* 2010; 2: 26.

30. Nannelli G, Terzuoli E, Giorgio V, et al. ALDH2 activity reduces mitochondrial oxygen reserve capacity in endothelial cells and induces senescence properties. *Oxid Med Cell Longev* 2018; 2018: 9765027.
31. Berry BJ and Kaeberlein M. An energetics perspective on geroscience: mitochondrial protonmotive force and aging. *Geroscience* 2021; 43: 1591–1604.
32. Lourenco CF, Ledo A, Barbosa RM, et al. Neurovascular-neuroenergetic coupling axis in the brain: master regulation by nitric oxide and consequences in aging and neurodegeneration. *Free Radic Biol Med* 2017; 108: 668–682.
33. Cao P, Zhang J, Huang Y, et al. The age-related changes and differences in energy metabolism and glutamate-glutamine recycling in the d-gal-induced and naturally occurring senescent astrocytes in vitro. *Exp Gerontol* 2019; 118: 9–18.
34. Hipkiss AR. Aging, Alzheimer's disease and dysfunctional glycolysis; similar effects of too much and too little. *Aging Dis* 2019; 10: 1328–1331.
35. Dick AP, Harik SI, Klip A, et al. Identification and characterization of the glucose transporter of the blood-brain barrier by cytochalasin B binding and immunological reactivity. *Proc Natl Acad Sci U S A* 1984; 81: 7233–7237.
36. Huang Y, Lei L, Liu D, et al. Normal glucose uptake in the brain and heart requires an endothelial cell-specific HIF-1 α -dependent function. *Proc Natl Acad Sci USA* 2012; 109: 17478–17483.
37. Bae S, Choi Y, Choi H, et al. Single-cell analysis reveals the key role of enhanced endothelial glucose uptake in neurometabolic coupling. *J Nucl Med* 2020; 61: 85–85.
38. Barros LF, San Martín A, Ruminot I, et al. Near-critical GLUT1 and neurodegeneration. *J Neurosci Res* 2017; 95: 2267–2274.
39. Seidner G, Alvarez MG, Yeh JI, et al. GLUT-1 deficiency syndrome caused by haploinsufficiency of the blood-brain barrier hexose carrier. *Nat Genet* 1998; 18: 188–191.
40. McCall AL, Van Bueren AM, Nipper V, et al. Forebrain ischemia increases GLUT1 protein in brain microvessels and parenchyma. *J Cereb Blood Flow Metab* 1996; 16: 69–76.
41. Winkler EA, Nishida Y, Sagare AP, et al. GLUT1 reductions exacerbate Alzheimer's disease vasculo-neuronal dysfunction and degeneration. *Nat Neurosci* 2015; 18: 521–530.
42. Abdul Muneer PM, Alikunju S, Szlachetka AM, et al. Impairment of brain endothelial glucose transporter by methamphetamine causes blood-brain barrier dysfunction. *Mol Neurodegener* 2011; 6: 23.
43. Jais A, Solas M, Backes H, et al. Myeloid-cell-derived VEGF maintains brain glucose uptake and limits cognitive impairment in obesity. *Cell* 2016; 166: 1338–1340.
44. Alique M, Sanchez-Lopez E, Bodega G, et al. Hypoxia-inducible factor-1 α : the master regulator of endothelial cell senescence in vascular aging. *Cells* 2020; 9: 195.
45. Doddaballapur A, Michalik KM, Manavski Y, et al. Laminar shear stress inhibits endothelial cell metabolism via KLF2-mediated repression of PFKFB3. *Arterioscler Thromb Vasc Biol* 2015; 35: 137–145.
46. Xu Y, An X, Guo X, et al. Endothelial PFKFB3 plays a critical role in angiogenesis. *Arterioscler Thromb Vasc Biol* 2014; 34: 1231–1239.
47. He X, Zeng H, Chen ST, et al. Endothelial specific SIRT3 deletion impairs glycolysis and angiogenesis and causes diastolic dysfunction. *J Mol Cell Cardiol* 2017; 112: 104–113.
48. Burmistrova O, Olias-Arjona A, Lapresa R, et al. Targeting PFKFB3 alleviates cerebral ischemia-reperfusion injury in mice. *Sci Rep* 2019; 9: 11670.
49. Liu J. Poststroke angiogenesis: blood, bloom, or brood? *Stroke* 2015; 46: e105-106–e106.
50. Mooradian AD. Effect of aging on the blood-brain barrier. *Neurobiol Aging* 1988; 9: 31–39.
51. Yan X, Hu Y, Wang B, et al. Metabolic dysregulation contributes to the progression of Alzheimer's disease. *Front Neurosci* 2020; 14: 530219.
52. Reutzel M, Grewal R, Dilberger B, et al. Cerebral mitochondrial function and cognitive performance during aging: a longitudinal study in NMRI mice. *Oxid Med Cell Longev* 2020; 2020: 4060769.
53. Navarro A and Boveris A. Brain mitochondrial dysfunction in aging: conditions that improve survival, neurological performance and mitochondrial function. *Front Biosci* 2007; 12: 1154–1163.
54. Kiss T, Balasubramanian P, Valcarcel-Ares MN, et al. Nicotinamide mononucleotide (NMN) treatment attenuates oxidative stress and rescues angiogenic capacity in aged cerebrovascular endothelial cells: a potential mechanism for the prevention of vascular cognitive impairment. *Geroscience* 2019; 41: 619–630.
55. Kiss T, Nyul-Toth A, Balasubramanian P, et al. Nicotinamide mononucleotide (NMN) supplementation promotes neurovascular rejuvenation in aged mice: transcriptional footprint of SIRT1 activation, mitochondrial protection, anti-inflammatory, and anti-apoptotic effects. *Geroscience* 2020; 42: 527–546.
56. Newsholme P, Procopio J, Lima MM, et al. Glutamine and glutamate – their central role in cell metabolism and function. *Cell Biochem Funct* 2003; 21: 1–9.
57. Hincsa SB, Salcedo C, Wagner A, et al. Brain endothelial cells metabolize glutamate via glutamate dehydrogenase to replenish TCA-intermediates and produce ATP under hypoglycemic conditions. *J Neurochem* 2021; 157: 1861–1875.
58. Chen Q, Kirk K, Shurubor YI, et al. Rewiring of glutamine metabolism is a bioenergetic adaptation of human cells with mitochondrial DNA mutations. *Cell Metab* 2018; 27: 1007–1025.e1005.
59. Ferrari F, Gorini A, Hoyer S, et al. Glutamate metabolism in cerebral mitochondria after ischemia and post-ischemic recovery during aging: relationships with brain energy metabolism. *J Neurochem* 2018; 146: 416–428.